Journal of the Korean Physical Society, Vol. 31, No. 1, July 1997, pp. 127∼130

Low Temperature Scanning Tunneling Microscopy/Spectroscopy Study of Two Different Layers In Poly-Type 4*Hb*-TaS_2 at 4.2 K

Ju-Jin Kim

Department of Physics, Chonbuk National University, Chonju 561-756

Håkan Olin

Department of Physics, Chalmers University of Technology, S-412 96 Göteborg, Sweden

(Received 10 January 1997)

Using scanning tunneling microscope (STM), we have fabricated steps of $4Hb$-TaS_2 with the height $\sim$ 6 Å and investigated the electronic and atomic structures on the two different layers near the step region at 4.2 K. The measured STM images and tunneling spectra revealed completely different atomic and electronic structures of the $1T$ and $1H$ type layers. The $1T$ type layers showed the typical $\sqrt{13}\times\sqrt{13}$ charge-density-wave (CDW) structures showing insulating behaviors, whereas the $1H$ type layers showed metallic behaviors and had the triangular atomic structure with a very weak 3×3 CDW superlattice at a low bias voltage and with a superposed $\sqrt{13}\times\sqrt{13}$ CDW superlattice at a high positive bias voltage. The bias dependent STM image on the surface of $1H$ layer can be explained by the energy dependent tunneling process between STM tip and a stack of metallic $1H$ layer and insulating $1T$ layer.

The poly-type $4Hb$-TaS_2 is composed of alternating layers of octahedral co-ordination ($1T$) and trigonal prismatic co-ordination ($1H$). Many studies on this material, particularly, related to the charge density wave (CDW) have been done using electron diffraction [1], resistivity measurements [2–4], and more recently scanning tunneling microscope (STM) [5]. This alternating layer structure gives interesting atomic and electrical properties which were understood as a composite nature of those observed in the pure octahedral such as $1T$-TaS_2 and the trigonal prismatic phases such as the $2H$-TaS_2. Each layer is also believed to maintain its characteristic features found in the corresponding pure phases, although there is a small electron transfer between the two different layers [6].

According to the scanning tunneling microscope studies by Giambattista *et al.* [7] and Coleman *et al.* [5], the poly-type $4Hb$-TaS_2 has completely different kinds of images on the two opposite faces of the same crystal cleave; one kind with a $\sqrt{13}\times\sqrt{13}$ CDW and another kind with atomic structures, presumably representing the $1T$-type and $1H$-type layers. Recently, Han *et al.* [8] observed strong bias dependent STM images at room temperature. A fully developed $\sqrt{13}\times\sqrt{13}$ CDW was observed even on the presumably $1H$ surface at relatively high positive bias voltage. Therefore, it is very important to identify each layer precisely, that is, whether the top layer is $1T$ or $1H$.

In this study, we have fabricated steps of $4Hb$-TaS_2 with the height $\sim$ 6 Å using a layer-by-layer etching technique [9,10] and investigated the electronic and atomic structures on the two different layers near the step region at 4.2 K. The measured STM images and tunneling spectra revealed completely different atomic and electronic structures of the $1T$ and $1H$ type layers. The $1T$ type layers showed the typical $\sqrt{13}\times\sqrt{13}$ CDW structures, whereas the $1H$ type layers had the triangular atomic structure with a weak 3×3 CDW superlattice at a low bias voltage and with a superposed $\sqrt{13}\times\sqrt{13}$ CDW superlattice at a high positive bias voltage. The measured tunneling spectra on each layer at 4.2 K also showed entirely different characteristics between the two layers near the step; the $1H$ layer showed the metallic behavior, whereas the $1T$ layer showed an opening of the wide insulating gap structures at the Fermi level at 4.2 K.

Single crystals of $4Hb$-TaS_2 were grown by the usual iodine transport method. The samples were cleaved at room temperature in air and set in the STM unit, which was placed in the center of a doubly shielded cryostat in a He exchange gas environment. The STM unit was cooled very slowly to 4.2 K for low temperature experiments. Mechanically polished Pt/Ir tips were used. All images were obtained in the constant current mode.

Figure 1(a) shows a perspective view of STM image (445 Å × 445 Å) of the $4Hb$-TaS_2 single crystal at 4.2 K exhibiting a step structure. The tunneling current and

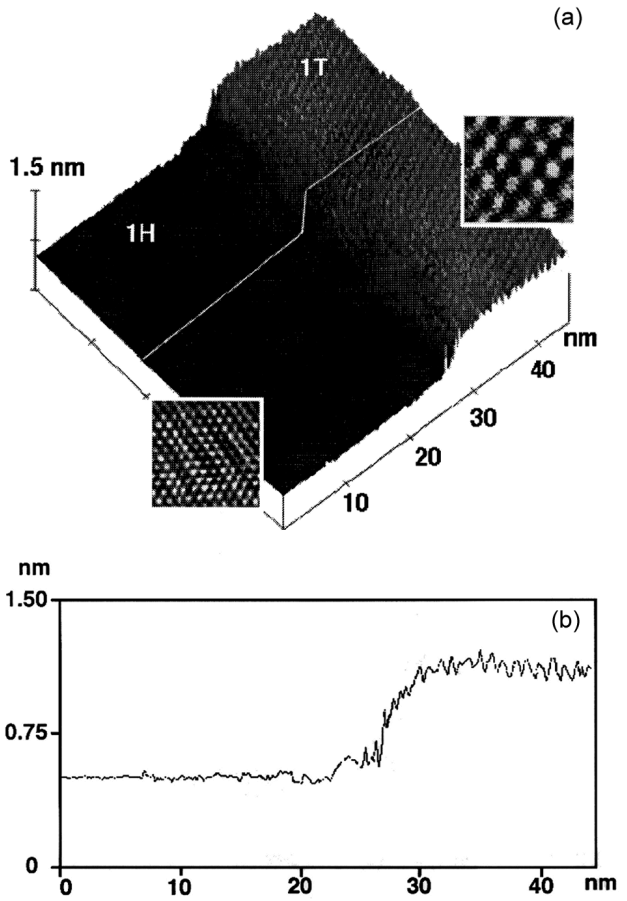

Fig. 1. (a) Perspective view of STM image of $4Hb$-TaS_2 near the step region after one molecular layer etching at 4.2 K. Zoom pictures at $1T$ layer and $1H$ layer show the typical $\sqrt{13} \times \sqrt{13}$ CDW and weak 3×3 CDW modulations, respectively. (b) The cross sectional profile noted by the white straight line in the STM image. The step height was estimated to ~ 6 Å.

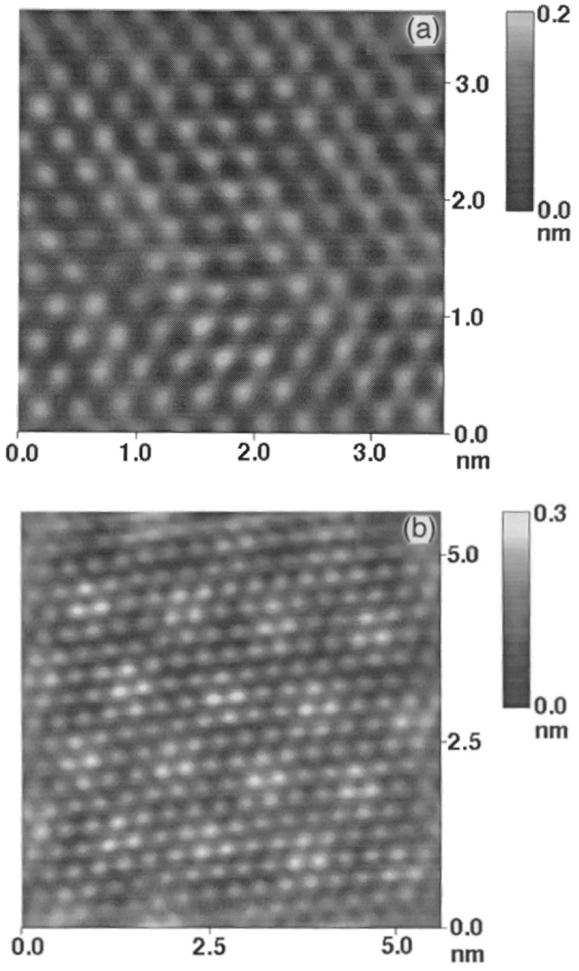

Fig. 2. (a) STM image on the lower layer in Fig. 1(a) with a bias voltage –50 mV. (b) STM image on the lower layer in Fig. 1(a) with a high positive bias voltage 300 mV.

bias voltage were 5 nA and 100 mV, respectively. Originally, this area consisted of a flat surface with a strong modulation of $\sqrt{13} \times \sqrt{13}$ CDW superlattice presumably corresponding to the $1T$ phase. Due to the weak van der Waals force between each layer in the transition metal dichalcogenides, it is possible to etch away individual layers using STM tip [9,10] in a well defined manner. Using this technique, it should be possible to choose different layers in the poly-type transition metal dichalcogenides by making new clean layers. This also enable one to study the atomic and electronic structures on the two different layers precisely in the same tunneling condition. By making a continuos scanning process with a relatively small tunneling resistance on the specified area, we could remove the lower part of layer as shown in Fig. 1(a) using a layer-by-layer etching method. Fig. 1(b) shows the cross sectional profile along the line indicated by the white line in Fig. 1(a). The step height was estimated to about 6 Å which is equivalent to the lattice constant along the c-axis within experimental error. It shows that the step is made up of one S-Ta-S molecular layer [1, 5]. This kind of etching method allows us to clearly distinguish between the two type of layers that exist. The STM image near the boundary region shows clearly two regions separated by a step. The upper layer shows a strong modulation with a periodicity ≈ 12 Å whereas rather a flat surface with traces of atomic structures is visible in the lower layer. The $\sqrt{13} \times \sqrt{13}$ CDW superlattice is clearly resolved in the upper layer corresponding to the $1T$ layer. However, the lower layer shows an atomic structure with a lattice constant ≈ 3 Å believed to be the $1H$ layer.

To study the more detailed structures on two different layers, we measured STM images with a small scan area on the surface of two different layers. The STM image of

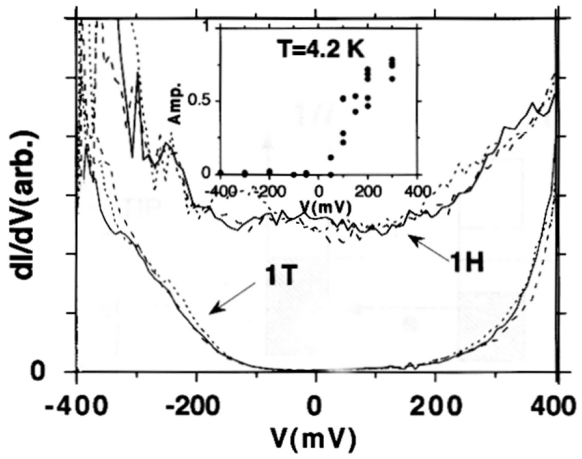

Fig. 3. Tunneling spectra at 4.2 K measured on the upper layer and the lower layer. The current and bias voltage were 1 nA [0.5 nA] and 100 mV [100 mV] on the upper [lower] layer. Inset: the intensity of $\sqrt{13} \times \sqrt{13}$ CDW modulation in $1H$ layer as a function of bias voltage at 4.2 K. Intensity is normalized at a high bias voltage.

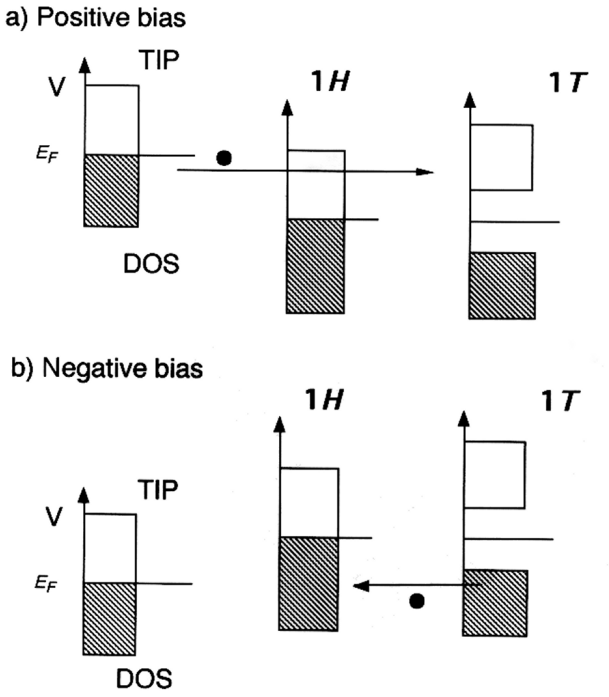

Fig. 4. The schematic tunneling processes between tip and a stack of metallic $1H$ and insulating $1T$ layer based on the measured tunneling spectra at 4.2 K. At negative bias the tunneling from the $1T$ layer is suppressed by the barrier due to the occupied states in the $1H$ layer.

the upper layer in Fig. 1(a) at 4.2 K showed the typical $\sqrt{13} \times \sqrt{13}$ CDW modulation with a small atomic modulations. In the low bias voltage, we have also observed the $\sqrt{13} \times \sqrt{13}$ CDW modulation with a relatively large z deflection $\sim$ 3.5 Å though the amplitude of the CDW modulation decreased with increasing a bias voltage, we could observe $\sqrt{13} \times \sqrt{13}$ CDW structures in this layer over the whole voltage region measured.

However, in the lower layer, we obtained strong bias dependent images. At low bias voltages below + $\sim$ 50 mV, we observed a very weak 3×3 CDW superlattice (Fig. 2(a)). Although the well developed 3×3 CDW structure was observed in the corresponding pure phase $2H$-TaS_2, this has not yet been observed in the $1H$ layer of $4Hb$-TaS_2 [5]. This would be related to much lower CDW onset temperature of $4Hb$-TaS_2 ($\sim$ 22 K) than that of the corresponding pure phase ($\sim$ 75 K) [4,11]. At a relatively high positive bias voltage larger than $\sim$ 100 mV, we observed completely different kind of CDW patterns, that is, a $\sqrt{13} \times \sqrt{13}$ CDW modulation which arise from the second $1T$ layer (Fig. 2 (b)) with the clear surface S atomic structures. For the negative bias voltage, there is no appreciable $\sqrt{13} \times \sqrt{13}$ CDW spot. The intensity of $\sqrt{13} \times \sqrt{13}$ CDW in $1H$ layer was estimated from the corresponding six spots in Fourier transform of the STM images. As the bias increases from the negative to positive, $\sqrt{13} \times \sqrt{13}$ CDW modulation starts to appear around 50 mV and increases as shown in Inset of Fig. 3. This kind of bias dependency of STM images is believed to be due to an energy dependent tunneling process between $1T$ and $1H$ layer [8]. Hence it is indispensable to know the detailed nature of the density of states in $1T$ and $1H$ layers near the Fermi level to understand the bias dependent STM image.

To clarify the bias depenent STM image, we have also measured the tunneling spectra on the surface of two different layers at 4.2 K. Fig. 3 shows the tunneling spectra measured on the surface of $1T$ and $1H$ layers, respectively. The tunneling spectra at the $1T$ layer show an opening of a wide gap about 600-700 mV exhibiting evident insulating nature of this layer. According to photo electron spectroscopy study [12,13] and tunneling experiment [14], $1T$-TaS_2 in the commensurate phase experiences a Mott transition at the nearly commensurate-commensurate transition point (140 K $\sim$ 180 K) as lowering the temperature. The insulating nature in the commensurate $1T$-TaS_2 was interpreted as an opening of the Mott gap [12–14]. Moreover the $1T$ layer in the poly type $4Hb$-TaS_2 is believed to have the almost same properties as the commensurate $1T$-TaS_2 [6]. Hence it is believed that the insulating gap in $1T$ layer of the $4Hb$-TaS_2 also originate from the Mott localization, not the CDW transition. Whereas the tunneling spectra at the $1H$ layer show a metallic character with a finite DOS at the Fermi level unlike the $1T$ layer. Although Coleman *et al.* estimate the CDW gap from the weak structure of the tunneling spectra in $1H$ layer as smaller than 30 meV, the CDW structure in $1H$ layer has not yet been

resolved clearly [11]. In our tunneling spectra, the existence of the CDW gap is also not clear although the overall shape of tunneling spectra is similar to that of the spectra of $2H$-TaS_2 by Wang *et al.* [15].

The imaging of a $\sqrt{13} \times \sqrt{13}$ CDW on the surface of $1H$ layer is only possible due to an electron tunneling from the tip through the upper $1H$ layer to the second $1T$ layer. Figure 4 shows the schematic tunneling processes based on our tunneling spectra. It shows two different tunneling processes between the tunneling tip and a stack of the metallic $1H$ and insulating $1T$ layer at positive and negative biases. At a positive bias the tunneling into the $1T$ unoccupied states occurs through the empty states of the surface $1H$ layer. However, at a negative bias the tunneling from the $1T$ layer apparently suppressed because electrons should overcome the barrier due to the occupied states of $1H$ layer as shown in Fig. 4. The bias dependency of the STM image on the surface of $1H$ layer reflects the difference in the intrinsic band structures of two layers. From our tunneling spectra on the $1T$ layer (Fig. 3), we can roughly estimate the onset voltage of $\sqrt{13} \times \sqrt{13}$ CDW modulations as about 100 mV.

In summary, we have investigated the electronic and atomic structures at 4.2 K on the two different layers of $1T$ and $1H$ type near the step region prepared by the layer-by-layer etching technique. The measured STM images and tunneling spectra revealed clearly different atomic and electronic structures of the $1T$ and $1H$ type layers. The $1T$ type layers showed the typical $\sqrt{13} \times \sqrt{13}$ CDW structures, whereas the $1H$ type layers had the bias dependent STM images; the triangular atomic structure with a $\sqrt{13} \times \sqrt{13}$ CDW superlattice at a low bias voltage and with a superposed $\sqrt{13} \times \sqrt{13}$ CDW superlattice at a high positive bias voltage. The measured tunneling spectra on each layer at 4.2 K also showed entirely different electronic structures between the two layers near the step; the $1H$ layer showed the metallic behavior, whereas the $1T$ layer showed an opening of the wide insulating gap structures at the Fermi level at 4.2 K. The bias dependent STM image in the $1H$ layer turned out to originate from the difference in the intrinsic band structures of two layers.

ACKNOWLEDGMENTS

This work was supported by the Swedish Research Council for Engineering Science (TFR) and Chonbuk National University. We would like to thank Dr. Hans Starnberg and Prof. F. Levy for providing us with the single crystals.

REFERENCES

[1] J. A. Wilson, F. J. DiSalvo and S. Mahasan, Adv. Phys. **24**, 117 (1975).
[2] F. J. Di Salvo, B. J. Bagley, J. M. Voorhoeve and J. V. Waszczak, J. Phys. Chem. Solids **34**, 1357 (1973).
[3] W. J. Wattamaniuk, J. P. Tidman and R. F. Frindt, Phys. Rev. Lett. **35**, 62 (1975).
[4] R. H. Friend, D. Jerome, R. F. Frind and A. J. Yoffe, J. Phys. **C10**, 1013 (1977).
[5] R. V. Coleman, B. Giambattista, P. K. Hansma, A. Johnson, W. W. McNairy and C. G. Slough, Adv. Phys. **37**, 559 (1988).
[6] N. J. Doran, G. Wexler and A. M. Woolley, J. Phys. **C11**, 2967 (1978).
[7] B. Giambattista, A. Johnson, W. W. McNairy, C. G. Slough and R. V. Coleman, Phys. Rev. **B38**, 3545 (1988).
[8] W. Han, E. R. Hunt, O. Pankratov and R. F. Frindt, Phys. Rev. **B50**, 14746 (1994).
[9] B. Parkinson, J. Am. Chem. Soc. **112**, 7498 (1990).
[10] A. P. Volodin and J. Aarts, Physica **C235**, 1909 (1994).
[11] R. V. Coleman, Z. Dai, W. W. McNairy, C. G. Slough and C. Wang, in *Scanning Tunneling Microscopy*, edited by J. A. Stroscio and W. J. Kaiser (Academic Press, San Diego, 1993).
[12] R. Manzke, T. Buslaps, B. Pfalzgraf, M. Skibowski and O. Anderson, Europhys. Lett. **8**, 195 (1989).
[13] B. Dardel, M. Grioni, D. Malterre, P. Weibel, Y. Baer and F. Levy, Phys. Rev. **B45**, 1462 (1992).
[14] J.-J. Kim, W. Yamaguchi, T. Hasegawa and K. Kitazawa, Phys. Rev. Lett. **73**, 2103 (1994).
[15] C. Wang, C. G. Slough and R. V. Coleman, J. Vac. Sci. Technol. **B9**, 1048 (1991).